# Microscopic Insight into the Sputtering of Thin Polystyrene Films on Ag{111} Induced by Large and Slow Ar Clusters

**Lukasz Rzeznik,[†] Bartlomiej Czerwinski,[†] Barbara J. Garrison,[‡] Nicholas Winograd,[‡] and Zbigniew Postawa*,[†]**

*Smoluchowski Institute of Physics, Jagiellonian University, ul. Reymonta 4, 30-059 Krakow, Poland, and Department of Chemistry, The Pennsylvania State University, 104 Chemistry Building, University Park, Pennsylvania 16802*

*Received: August 19, 2007; In Final Form: October 16, 2007*

Molecular dynamics computer simulations were employed to model the bombardment of Ag{111} covered with a monolayer of sec-butyl-terminated polystyrene tetramer (PS4) molecules by the impact of large and slow clusters. The investigated surface was bombarded with clusters composed of between hundreds to 29 000 Ar atoms having a very low kinetic energy per atom (0.1−40 eV). The sputtering yield of molecular species and their internal, angular, and kinetic energy distributions were analyzed. The simulations demonstrated quite clearly that the physics of ejection by these large and slow clusters is distinct from the ejection events stimulated by the popular SIMS clusters, $C_{60}$, $Au_3$, and $SF_5$.

## 1. Introduction

Desorption stimulated by cluster projectiles has become an important process in organic and biological mass spectrometry since it was found a few years ago that the sputtering yields can be enhanced when an atomic projectile is replaced by a cluster ion with the same incident energy.[1,2] However, various degrees of enhancement of high mass secondary ions have been reported, depending upon the type of projectile, target material, and matrix. For example, thin polymer films on Ag do not seem to benefit from the use of polyatomic projectiles, while SIMS spectra from bulk polymers were dramatically improved.[3] There are also reports that cluster ion beams, $C_{60}^+$ in particular, lead to smaller damage accumulation in bombarded organic solids, which allows for depth profiling of molecular solids.[4−9] A wide range of clusters ranging from $Au_3$ to micrometer-sized droplets has been tested in a quest to find the optimum size of the cluster projectile.

Apart from numerous experiments, a significant theoretical effort has been performed to investigate how the mechanism of molecular desorption changes as the size of the projectile increases.[10−25] Computer simulations demonstrate that there is a significant difference between processes initiated by atomic and cluster projectiles. For monatomic projectiles, most of the primary energy is deposited deep inside the material and cannot contribute to ejection.[14,15,21] On the other hand, for cluster projectiles, the primary kinetic energy is partitioned between many constituent atoms as the projectile breaks up upon impact. The energy of individual atoms is, therefore, low, which results in a small penetration. As a consequence, the primary energy is deposited near the surface, and the ejection is very efficient. A limited penetration depth and a large sputtering yield are believed to be responsible for the improved depth profiling capabilities of cluster beams, as the damage induced by projectile impact is immediately removed.

* Corresponding author. E-mail: zp@castor.if.uj.edu.pl; tel.: (4812) 663-5626.

[†] Jagiellonian University.

[‡] The Pennsylvania State University.

While many theoretical studies have been reported for systems bombarded by small clusters,[10−13,16−18,20−24,26−29] much less is known about phenomena taking place during massive cluster bombardment. In pioneering experiments with massive glycerol clusters, Mahoney and co-workers have shown that desorption of large peptide and protein ions is possible.[30,31] Unfortunately, the ion beam is very unstable in these measurements, and the ion source becomes contaminated after a few hours and must be cleaned. Extensive sputtering of molecular products also has been observed in experiments in which singly charged water clusters $H^+(H_2O)_n$ with $n$ up to 3000 were used as projectiles.[32] However, also in this case, the ion source is difficult to control. In recent years, more stable ion sources of large cluster projectiles have been developed. Clusters composed of hundreds of Au atoms have been used to stimulate the ejection of organic material.[33,34] Even larger clusters composed of thousands of noble-gas atoms produced by supersonic expansion of high-pressure gas through a nozzle have been used in the processing and SIMS analysis of semiconductor materials.[35−38] Finally, very large, electrosprayed droplets of water and other organic solvents have been utilized for the desorption of analyzed material in electrospray droplet impact (EDI)[39] and desorption electrospray ionization (DESI)[40,41] mass spectrometries. While very gentle interactions are applied to desorb/ionize the sample under atmospheric pressure in DESI, high-momentum collisions taking place in a vacuum between the projectile atoms and the solid sample are used in EDI.

Two different modeling schemes have been applied to investigate the processes induced by large clusters. The first approach involves fluid-dynamics calculations.[42] In this technique, analytical equations of hydrodynamics are applied to describe the flow of a liquid medium. Although these calculations show very clearly the shock formation and jetting at the edge of the droplet, incorporation of explicit molecules is not possible. Another approach employs atomistic simulations to describe phenomena associated with the cluster impact.[22,35,43−46] Although the cluster size in these simulations has to be much smaller than for the fluid-dynamics approach, these simulations

10.1021/jp076667q CCC: $40.75 
Published on Web 12/15/2007 PAGE EST: 10.6

allow atomistic phenomena such as cluster fragmentation and internal excitation to be incorporated into the model.

Most theoretical research has concentrated on processes taking place inside the primary cluster since thermofluidics of liquid impact onto a rigid surface is important to many technological applications, such as the cleaning of surfaces, spray cooling, and ink-jet printing. These studies demonstrate that the cluster ion is deformed upon impact and that a high-density, high-pressure region is formed at the sample/cluster interface. The stress accumulated in this region is released by propagation of a shock-wave and by a side jetting or splashing of projectile atoms, followed by a slow volume expansion of a flattened cluster.[42,43,45]

Another group of studies has focused on the events taking place in bombarded materials.[22,35,44,46] These studies show that ejection characteristics depend strongly on the size and kinetic energy of a projectile. Contrary to small cluster bombardment, both the total energy of the projectile and the kinetic energy of an individual atom composing the cluster are considered important factors. If both energies are large, the processes initiated by cluster impact are very similar to the processes stimulated by high-energy small cluster bombardment. The emission of a sample material is strong, and a crater is formed in the bombarded material.[35,44,46] In contrast to small cluster bombardment, the impact of large particles can stimulate ejection also by very gentle interactions. For instance, in DESI, the molecules are removed by an impact of micrometer-sized droplets composed of particles having kinetic energy in the sub-millielectronvolt energy range.[40,41] Such energy is too low to stimulate ejection by individual molecule−molecule collisions. This observation indicates that collective processes have to be involved. It is currently accepted that splashing and/or a droplet pick-up followed by a subsequent ionization by electrospray-like mechanisms is responsible for molecular ejection occurring in this case.[40,41]

All of the atomistic studies performed to date on large cluster bombardment of solids have been performed for clean inorganic surfaces.[22,35,44,46] There are no simulations that investigate the processes induced by a large cluster impact in organic overlayers or molecular solids. In this study, we desired to push the limits of molecular dynamics computer simulations to the largest clusters to see what kind of new desorption mechanisms could emerge. The model system is a monolayer of polystyrene tetramers deposited on a metal substrate, as it has been found that no enhancement of molecular ejection is observed on thin organic overlayers with small clusters. The sample was bombarded by slow and large cluster projectiles composed of thousands of noble-gas atoms. Results indicate that the ejection of organic molecules can be very efficient and that the emission characteristics are distinctly different from those stimulated by atomic or small cluster impacts.

## 2. Model Details

Molecular dynamics (MD) computer simulations were utilized to elucidate the ejection mechanism of sec-butyl-terminated polystyrene tetramer (PS4) molecules on Ag{111}. The details of the computational procedure can be found elsewhere.[47] Briefly, the motion of the particles was determined by integrating Hamilton's equations of motion.[47] The forces among the atoms are described by a blend of empirical pairwise additive and many-body potential energy functions. The Ag−Ag interactions are described by the MD/Monte Carlo corrected effective medium (MD/MC-CEM) potential for fcc metals.[48] The Ar−C and Ar−H interactions are described using the purely repulsive KrC pairwise additive potential.[49] The interaction between Ar atoms as well as interactions between Ar and Ag atoms is described by a Lennard-Jones potential splined with KrC potential to properly describe high-energy collisions.[50] The adaptive intermolecular potential, AIREBO, developed by Stuart and co-workers is used to describe the hydrocarbon interactions.[51] This potential is based on the reactive empirical bond-order (REBO) potential developed by Brenner et al. for hydrocarbon molecules.[52] Finally, the interaction of C and H atoms with Ag atoms is described by a Lennard-Jones potential using established parameters.[53]

Two models approximating the Ag{111} substrate were used depending upon the cluster size and its kinetic energy. A smaller model consisting of a finite microcrystallite containing 166 530 Ag atoms arranged in 39 layers of 4270 atoms each was used for projectiles up to $Ar_{872}$ as well as $Ar_{2953}$ projectiles with a kinetic energy up to 5 eV/atom. This system is too small for other projectiles and was replaced by a larger system containing 611 442 atoms arranged in 39 layers of 15 678 atoms each. The sample size (175 Å × 175 Å × 90 Å for a smaller system and 337 Å × 334 Å × 90° Å for a larger system) was chosen to minimize edge effects associated with the dynamical events leading to the ejection of particles. Organic overlayers were represented by a monolayer of sec-butyl-terminated polystyrene tetramers (PS4) deposited on the surface of the Ag crystal. The smaller system contains 112 PS4 molecules, while 448 molecules are deposited on the larger system. Projectiles of $Ar_n$ ($n$ = 101, 202, 366, 872, 2953, 9000 and 27953) clusters were directed normal to the surface with a kinetic energy between 0.1 and 40 eV per atom. The projectile clusters have an amorphous structure. They were created by cutting out a roughly spherical cluster containing exactly $n$ atoms from the amorphous bulk structure. The cluster was relaxed before the simulation was initiated. Since it is known that statistical accuracy increases with cluster size,[20,27,28] a single trajectory was calculated for most impacts. A total of 20 trajectories was calculated in cases where internal, kinetic energy, and angular spectral distributions were evaluated. Each trajectory was initiated with a fresh sample with all atoms in their equilibrium minimum energy positions. The atoms in the target initially had zero velocity. The atoms in the cluster projectile initially have no velocity relative to the center of mass motion. The trajectories were terminated after 36 ps. At this time, the sputtering yield was saturated, and the total energy of the most energetic particle remaining in the solid was much less than the binding energy of Ag (2.95 eV) or the binding energy of the PS4 overlayer (approximately 2.1 eV).

There are two aspects of the computational setup that require special care. First, large pressure waves[10,16,17,20,27] are generated by a cluster bombardment that could possibly cause artifacts if allowed to reflect from the boundaries of the sample. There are several approaches that allow us to remove artifacts associated with a possible reflection of these waves from the sides of the crystal.[20,54−57] In our simulations, a stochastic region at 0 K and a rigid layer were put on five sides of the crystal to eliminate this unwanted artifact.[20] Second, the definition of ejected species must be carefully examined due to the eruption of the material caused by the $Ar_n$ impact as shown in Figure 1. The implementation of the approaches to overcome these limitations has been previously described.[20]

The final computation issue to address is the stability of the ejected molecules. The PS4 molecules at the end of the trajectory, ∼36 ps, may have sufficient internal energy to dissociate before reaching a detector tens of microseconds later. It has been shown that removing the energized molecules is

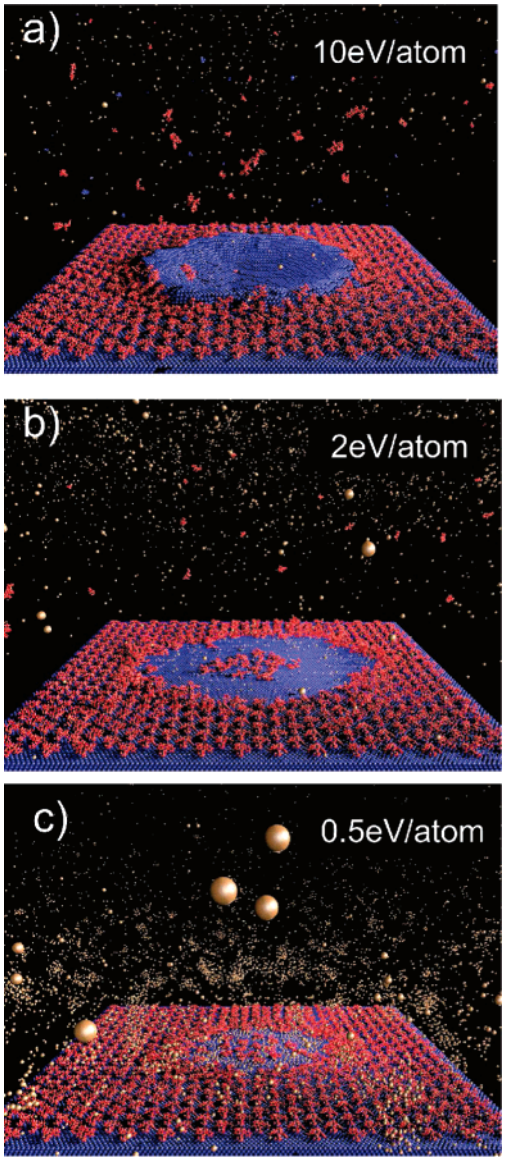


**Figure 1.** View of the PS4/Ag{111} system bombarded with $Ar_{9000}$ projectiles having a kinetic energy of (a) 10 eV, (b) 2 eV, and (c) 0.5 eV per atom at 36 ps after the ion impact. Polystyrene molecules, Ag atoms, and Ar atoms are depicted in red, blue, and peach, respectively.

required to obtain good agreement with experimental data.[15,58−60] One strategy for removing the clusters is to integrate their equations of motion for a sufficiently long time such that the likelihood of further dissociation is small.[58] This strategy is successful when the interaction potential is reliable for dissociation channels and when the decay time is less than $10^{-9}$ s. The application of this approach to the bombardment of a clean metal showed that there were changes to the cluster and monomer yields and energy distributions between a few picoseconds after the bombardment event to several hundreds of picoseconds later.[58,59]

An alternative strategy is to use a fixed cutoff value of the internal energy to determine which molecules will dissociate.[15,60] This approach for differently sized molecules is described in detail elsewhere. This strategy is best when the interaction potential is not sufficient for describing the dissociation pathways, as is the case here for the hydrocarbon species. The downside to this approach is that the effect of the dissociation events on the smaller decay products is not included.

For the simulations here, a constant value of internal energy was used to estimate as to whether a PS4 molecule will dissociate. The prescription for defining the internal energy was given previously.[15] Unimolecular decomposition theory predicts that more than 90% of PS4 molecules will be detected on a microsecond time scale[15] if their internal energy does not exceed 28 eV. Therefore, this value is used as a dissociation threshold.

## 3. Results and Discussion

The discussion begins with an overview of the basic collision events for $Ar_n$ bombardment as these events can provide the foundation for understanding the other properties. The ejection yields are discussed next, followed by the internal, kinetic energy, and angular distributions. Finally, a novel mechanism of molecular ejection is proposed and evaluated.

**Collision Events.** Snapshots of the PS4/Ag{111} system taken 36 ps after impact of the $Ar_{9000}$ projectiles having initial kinetic energies of 10, 2, and 0.5 eV per atom are shown in Figure 1. A significant portion of the PS4 overlayer is altered upon the impact of each projectile. At 10 eV/atom, most of the primary energy is deposited in a shallow volume of the metal substrate, leading to massive damage and the ejection of many particles. A large hemispherical crater is formed in the substrate. The physics of the crater formation and molecular ejection is the same as for energetic small cluster bombardment.[22,23,28] Because of the small thickness and openness of the PS4 monolayer, only a small portion of the primary energy is dissipated within the organic overlayer. The collisions between incoming Ar atoms and adsorbed organic molecules are more energetic than the strength of the chemical bonds. As a result, many emitted molecules are fragmented. As a consequence of cluster impact, organic molecules are ejected both by interaction with substrate and by projectile atoms as has been described elsewhere.[23,28] In this study, we focused on processes leading to molecular ejection initiated by projectiles with a kinetic energy not sufficient to eject substrate atoms. Such processes have not been investigated to date.

Ejection of substrate particles strongly decreases when the kinetic energy of the projectile is reduced. Surprisingly, the emission of PS4 molecules is much less influenced by a decrease of the primary kinetic energy. As shown in Figure 1b, at 2 eV/atom, Ag atoms are not emitted, and the substrate is virtually intact. At the same time, many PS4 molecules are still visible in the flux of ejected particles. These molecules are removed from a ring-like surface area. It is interesting to note that most of the molecules located below the cluster are neither relocated nor ejected at this energy. Finally, at 0.5 eV/atom, no ejection of PS4 molecules is observed, and the molecules are only relocated from their initial positions and pile up at the periphery of the altered ring-like area.

The snapshots displayed in Figure 1 represent a structure of the $Ar_{9000}$ irradiated systems at the final time frame of our simulations. A temporal evolution of collision events leading to the ejection of organic molecules due to $Ar_{9000}$ irradiation with a kinetic energy of 2 eV per atom is shown in Figure 2. All substrate atoms are removed from Figure 2 to allow for a better visualization of the PS4 molecules. The ejected molecules are colored according to their final kinetic energy as described in the caption. The evolution of a slow, large cluster projectile upon impact on the metallic and semiconductor substrate has already been investigated and will not be discussed here.[43,45] Briefly, the cluster ion is deformed upon impact, and a high-density, high-pressure region is formed at the sample/cluster interface. The stress accumulated in this region is released by propagation of a shock-wave and by a side jetting of projectile atoms, followed by a slow volume expansion of a flattened

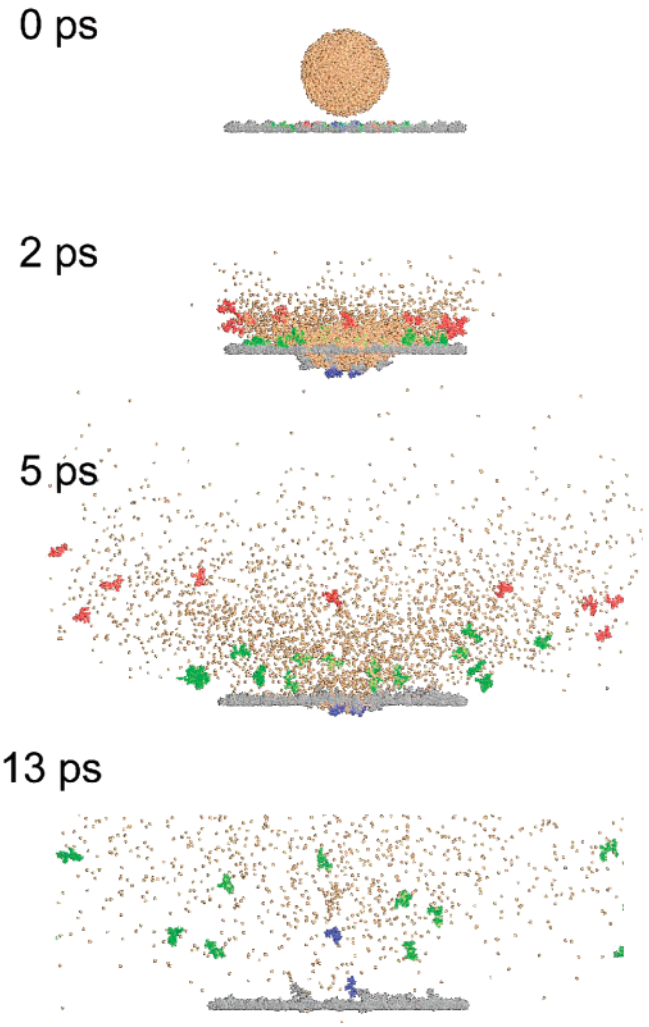


**Figure 2.** Side view of the temporal evolution of the collision events stimulated by 15 keV $Ar_{2953}$ impact at a PS4/Ag{111} system at normal incidence. All metal substrate atoms are removed from the pictures. Peach spheres depict Ar atoms. Ejected PS4 molecules with a total kinetic energy greater than 30 eV are depicted in red. Molecules emitted with a kinetic energy less than 30 eV but greater than 2 eV are in green, while the molecules with an energy less than 2 eV are depicted by blue spheres. Grey spheres depict PS4 molecules that were not sputtered from the surface.

cluster. Because the primary energy per atom is low and the mass of substrate atoms is much larger than the mass of projectile atoms, most of these atoms are backreflected into the vacuum.

The impact of a slow and massive cluster leads to a large deformation of the metallic substrate localized around the impact area as can be deduced from the snapshot taken at 2 ps. However, because the density of deposited energy is low, ejection of substrate atoms does not occur at this primary kinetic energy. Ultimately, the substrate restores itself to its original structure. In contrast to the studies performed with atomic and small cluster projectiles, many organic molecules are still ejected despite the fact that substrate atoms are not energized.[14,15,23,28] This result indicates that a different mechanism of molecular ejection operates in this regime. The animations of collision events as well as the snapshots presented in Figure 2 indicate that the molecules seem to be flushed away by a stream of side-jetting, backreflected Ar atoms. The data also indicate that molecular ejection is not uniform in time but that it has a wave-like structure that seems to be correlated with the kinetic energy

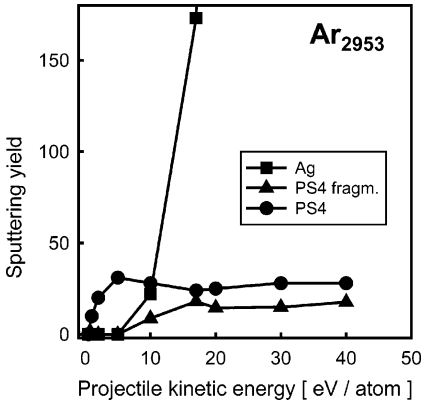


**Figure 3.** Dependence of the sputtering yields of silver atoms (squares) and fragmented (triangles) and intact (circles) PS4 molecules ejected from a PS4/Ag{111} system with the kinetic energy of the $Ar_{2953}$ projectile for normal incidence bombardment.

of emitted molecules. This phenomenon will be discussed in more detail in the section on kinetic energy distributions.

**Yields.** The sputtering yield dependence on the initial kinetic energy is shown in Figure 3 for $Ar_{2953}$ cluster impact at normal incidence. At a very low kinetic energy, no material is removed from the sample. As the energy exceeds approximately 1 eV per atom, the ejection of intact PS4 molecules is initiated, and the yield steeply increases with the kinetic energy. Up to approximately 5 eV per atom, only intact molecules are emitted. At a higher kinetic energy, the ejection of intact PS4 molecules saturates, while the ejection of molecular fragments and substrate atoms becomes visible. While the ejection of molecular fragments also saturates around 17 eV/atom, the sputtering yield of substrate atoms increases almost linearly with the primary kinetic energy above the energy threshold of approximately 10 eV/atom. The linear dependence of the sputtering yield on the primary kinetic energy above a certain threshold has been observed previously both experimentally and in computer simulations during cluster bombardment of inorganic and thick organic samples.[22,61,62] Such behavior is attributed to the primary energy being deposited almost entirely within a sample volume that contributes to the ejection.[62]

The ejection process stimulated by a large, noble-gas cluster impact can be quite efficient. As shown in Figure 3, the 15 keV $Ar_{2953}$ cluster leads to emission of 33 PS4 molecules. By comparison, barely four molecules are uplifted by a $C_{60}$ projectile having the same kinetic energy.[28] As a strong signal is always a beneficiary factor for SIMS/SNMS spectrometry, these characteristics could make large, slow Ar clusters potentially attractive for chemical analysis of organic samples. In particular, analysis of thin organic overlayers could benefit from large cluster projectiles since the application of small clusters is not effective at enhancing the yield when compared to atomic projectiles.[2] The data shown in Figure 3 were collected for the $Ar_{2953}$ projectile. However, identical trends were observed for other clusters investigated in this study. Only the threshold energy for desorption, the onset energy for yield saturation, and the total sputtering yields vary with the cluster size. For the same kinetic energy, the thresholds for desorption of all investigated particles shift toward a lower kinetic energy as the projectile size increases.

The sputtering yield of substrate and organic particles responds in a different way to the variation of the cluster size. As shown in Figure 4, the sputtering yield of substrate atoms monotonically decreases with increasing cluster size. A similar trend can be observed for fragmented molecules, although the

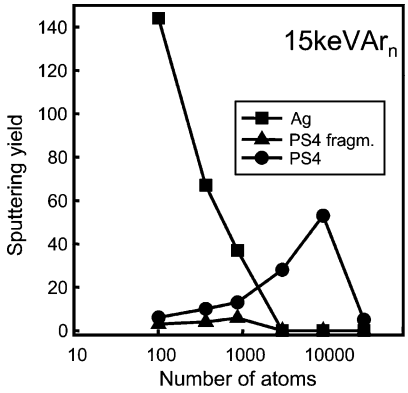


**Figure 4.** Dependence of the sputtering yields of silver atoms (squares) and fragmented (triangles) and intact (circles) PS4 molecules ejected from a PS4/Ag{111} system on the number of atoms composing a 15 keV cluster projectile.

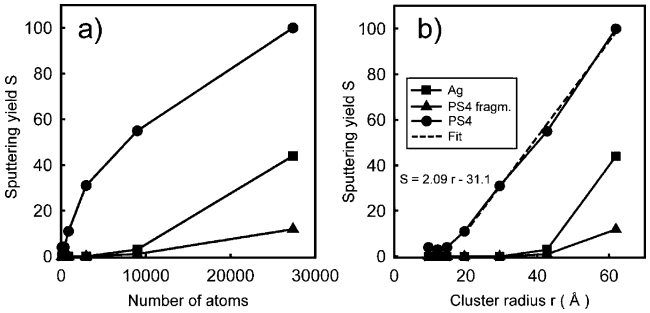


**Figure 5.** Dependence of the sputtering yields of silver atoms (squares) and fragmented (triangles) and intact (circles) PS4 molecules ejected from a PS4/Ag{111} system on (a) the number of atoms composing a projectile and (b) the radius of the projectile. The primary kinetic energy of the projectile is 5 eV/atom. The dashed line indicates a linear fit to the data for molecules composed of more than 200 atoms.

amount of signal variation is much smaller than for Ag. On the other hand, the yield of intact organic molecules has a non-monotonic behavior with a maximum around $Ar_{9000}$. A similar behavior of substrate atom and molecular ion emission has been observed experimentally by Ninomiya et al. for arginine molecules deposited on a silicon substrate bombarded with Ar cluster projectiles.[38]

For small Ar projectiles, each atom of the cluster has a relatively high kinetic energy. Consequently, projectile atoms can penetrate into the substrate, depositing their energy in a shallow volume located close to the surface. As a result, the integrity of the substrate is broken, and many atoms are ejected. These atoms can interact with the adsorbed molecules, leading to the emission of organic species by the same processes as observed during $C_{60}$ bombardment.[23,28] Because the projectile is small, it can directly interact only with a limited number of adsorbed PS4 molecules. Consequently, ejection of organic molecules is small. Furthermore, because atoms comprising the cluster are energetic, molecular fragmentation is the preferred reaction channel of such interactions. As the cluster size increases, the energy of individual atoms in the cluster decreases. At the same time, the impact area is larger. Both of these factors lead to a decrease in the spatial density of the primary energy and, consequently, to a decrease in both the substrate erosion and the molecular fragmentation. At a certain cluster size, projectile atoms do not have a sufficient kinetic energy to be able to penetrate into the substrate, and the ejection of Ag atoms ceases. The PS4 molecules are, however, still ejected, which indicates that the driving force for molecular ejection cannot originate from Ag−PS4 interactions but must arise from Ar−PS4 collisions. The yield of ejected intact molecules increases at first because the fragmentation decreases, and the area of possible Ar−PS4 interactions increases as the cluster size increases. At a critical size, however, a decrease in the kinetic energy carried by an individual Ar atom dominates over other effects, and the yield declines. Finally, the amount of energy transferred in Ar−PS4 collisions becomes so low that the ejection of PS4 molecules is no longer possible. In this case, only backreflected Ar atoms are detected above the surface.

The data presented in Figure 4 are somewhat complicated because the yield is influenced both by an increase of a number of atoms in the projectile and by a decrease of the kinetic energy available to each Ar atom. To decouple these two quantities, calculations were made whereby the energy per atom was kept constant. The results are shown in Figure 5 for the primary kinetic energy of 5 eV/atom. It is evident that under these experimental conditions, the sputtering yield of all particles increases with the increase of the cluster size. Moreover, it seems that starting with the $Ar_{366}$ cluster, the increase of the PS4 sputtering yield has almost a linear dependence on the cluster radius. Such a dependence implies that the diameter of the ring-like area contributing to molecular ejection should be proportional to the diameter of the projectile. The natural consequence of this observation for the application of large, slow clusters in SIMS/SNMS is a conclusion that the analysis should be carried out with the largest available clusters, provided that a constant energy per atom can be secured. The dependence of the incidence angle on the sputtering yield is also an important issue for SIMS/SNMS applications. Our calculations indicate that the signal only weakly depends on the incident angle.

**Internal Energy and Dissociation.** Another important factor for SIMS/SNMS mass spectrometry is the fragmentation of the analyzed molecules on their way from the surface to the detector. It has been shown that the amount of fragmentation is directly related to the internal energy of the ejected molecules. More internally excited molecules have a smaller probability of surviving.[15,60] The internal energy distributions of PS4 molecules collected at 36 ps after the 15 keV Ga, $C_{60}$, and $Ar_{2953}$ projectile impacts are calculated and presented in Figure 6 to evaluate the role of this phenomenon in our system. Most of the PS4 molecules ejected by 15 keV Ga have an internal energy lower than the assumed dissociation threshold of 28 eV.[15] On the other hand, ∼14 and ∼23% of molecules ejected by 15 keV $C_{60}$ and 15 keV $Ar_{2953}$ impact have internal energies exceeding the threshold value. All of these molecules will dissociate, and consequently, they will not be detected. The data indicate, however, that the internal energy is sensitive to the kinetic energy of the cluster projectile. As shown in Figure 6b, a decrease of the primary kinetic energy from 15 keV (5 eV/atom) to 12 keV (4 eV/atom) is sufficient to secure detection of almost all PS4 molecules.

**Kinetic Energy Distributions.** The kinetic energy distribution of ejected particles is a quantity that can be measured and, at times, can be used to help understand the mechanisms responsible for emission. Angle integrated kinetic energy distributions of PS4 molecules ejected due to 15 keV $Ar_{2953}$, 15keV Ga, and 15 keV $C_{60}$ projectiles are shown in Figure 7. The spectrum calculated for the impact of an Ar cluster contains all intact molecules collected 36 ps after the ion impact (solid line in Figure 7) and only the molecules with an internal energy lower than the assumed dissociation threshold (dashed line in Figure 7). As expected from studies on small cluster bombardment,[15,60] the high-energy portion of the spectrum is mainly modified when internally excited molecules are eliminated.

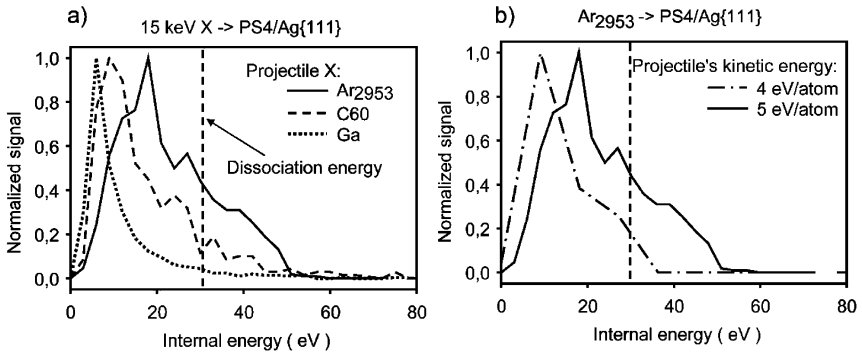


**Figure 6.** Peak normalized internal energy distributions of PS4 molecules ejected by (a) 15 keV $A_{2953}$ (solid line), 15 keV $C_{60}$ (dashed line), and 15 keV Ga (dotted line) bombardment and (b) 15 keV (solid line) and 12 keV (dashed line) $Ar_{2953}$ bombardment at normal incidence. The vertical dashed line is the cutoff energy used to determine which molecules will unimolecularly decay during the flight time to the detector.

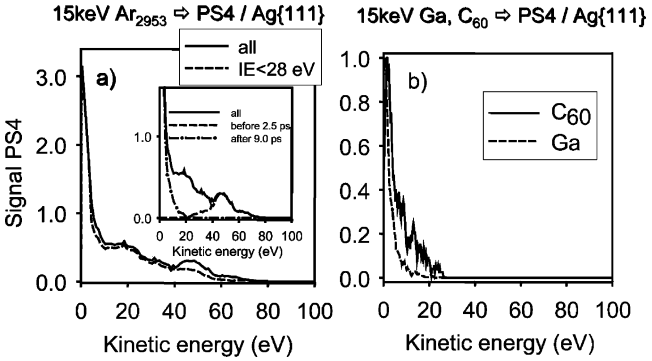


**Figure 7.** Angle-integrated kinetic energy distributions of intact PS4 molecules sputtered at normal incidence from PS4/Ag{111} by (a) 15 keV $Ar_{2953}$ for all internal energies (solid line) and for internal energies of less than 28 eV (dashed line) and (b) 15 keV $C_{60}$ (solid line) and 15 keV Ga (dashed line) at normal incidence. The inset in the left panel displays kinetic energy distributions of all PS4 molecules (solid line), PS4 molecules collected within 2.5 ps (dashed line), and molecules recorded later than 9 ps (dashed−dotted line) by a flat detector located 1 nm above the surface. The distributions shown in panel b are peak normalized.

The spectrum obtained for Ar cluster impact has several features that are not observed for small cluster projectiles. First, even though the kinetic energy per projectile atom is very low (5 eV/atom), many PS4 molecules are ejected with a very high kinetic energy. As shown in Figure 7b, the corresponding kinetic energy distributions of PS4 molecules ejected by 15 keV Ga and $C_{60}$ bombardment are much narrower. Most of the PS4 molecules are ejected with kinetic energies below 20 eV by both 15 keV Ga and $C_{60}$.[28] A second unexpected feature of the kinetic energy spectrum collected during 15 keV $Ar_{2953}$ impact is its complicated structure. Several peaks can be identified in the distribution stimulated by the $Ar_{2953}$ impact. The first peak occurs around 0.1 eV. Then, there is a peak near 20 eV, and finally, a third peak can be identified near 50 eV. It is also interesting to note that all these peaks can be correlated with the ejection time and original location of the molecules. As shown in the inset of Figure 7a, the molecules contributing to the peak at 50 eV are ejected very early, while low-energy molecules contributing to a peak near 0.1 eV are ejected very late. A similar conclusion can be also drawn from the data presented in Figure 2, where it is shown that the ejection of molecules having different kinetic energies is temporally correlated in a form of wave-like ejections. The first wave of ejected molecules is composed of molecules having a high kinetic energy. Then, ejection of medium-energy molecules contributing to the second peak is initiated. Finally, the slowest molecules are uplifted from the surface.

The final kinetic energy of ejected molecules can also be correlated with their initial locations relative to the point of the cluster impact. A top view of the original sample, bombarded by $Ar_{9000}$ having a kinetic energy of 5 eV/atom, is shown in Figure 8 with molecules colored according to their final kinetic energy. The coloring scheme was chosen to classify all molecules to one of the three peaks visible in the kinetic energy spectra. The most energetic molecules are initially located at the surface close to the perimeter of the cluster projectile. The final energy of ejected molecules decreases as they reside further away from the point of impact, although this trend only partially holds for molecules ejected with a very low kinetic energy. In this case, although some of the molecules are indeed located at the periphery of the interaction zone, there are also some molecules that are originally located directly underneath the impinging cluster. The data shown in Figure 8 were obtained for the $Ar_{9000}$ cluster projectile, but again, similar trends occur for all other investigated projectiles larger than $Ar_{202}$.

A comparison of the kinetic energy distributions calculated for 15 keV $C_{60}$ and 15 keV $Ar_{2953}$ projectiles indicates that the ejection of high-energy molecules cannot be explained by processes taking place during bombardment with clusters such as $C_{60}$, $Au_3$, or $SF_5$. As already mentioned, animations of the sputtering events indicate that high-energy molecules are being swept away by a flux of side-jetting Ar atoms. A similar concept of molecular entrainment was proposed in MALDI studies.[63] It would be interesting, therefore, to check as to whether this concept can explain our kinetic energy spectra. The entrainment mechanism postulates that all particles composing a flux of ejected material should have comparable velocities. Therefore, as the mass of PS4 molecules is almost 14 times larger than the mass of Ar atoms, the flux of Ar atoms having a kinetic energy of 5 eV per atom would entrain the PS4 molecules, accelerating them to a kinetic energy of approximately 70 eV. This value is, indeed, close to the energy of the most energetic peak visible in Figure 7a. However, this concept cannot explain why several peaks are present in the kinetic energy spectrum of ejected PS4 molecules.

**Angular Distributions.** The energy-integrated azimuthal and polar angle distributions of ejected Ar atoms and PS4 molecules are presented in Figure 9 for a 15 keV $Ar_{2953}$ projectile bombarding the PS4/Ag{111} system at normal incidence. Ejection of both Ar and PS4 is azimuthally isotropic. This isotropy breaks down, however, if the projectile arrives at the sample at an off-normal angle. In this case, most of PS4 molecules and Ar atoms are ejected in a specular azimuthal direction. The polar angle distributions presented in Figure 9b show that most of the Ar atoms and organic molecules are ejected at large polar angles. Ejection of off-normal organic

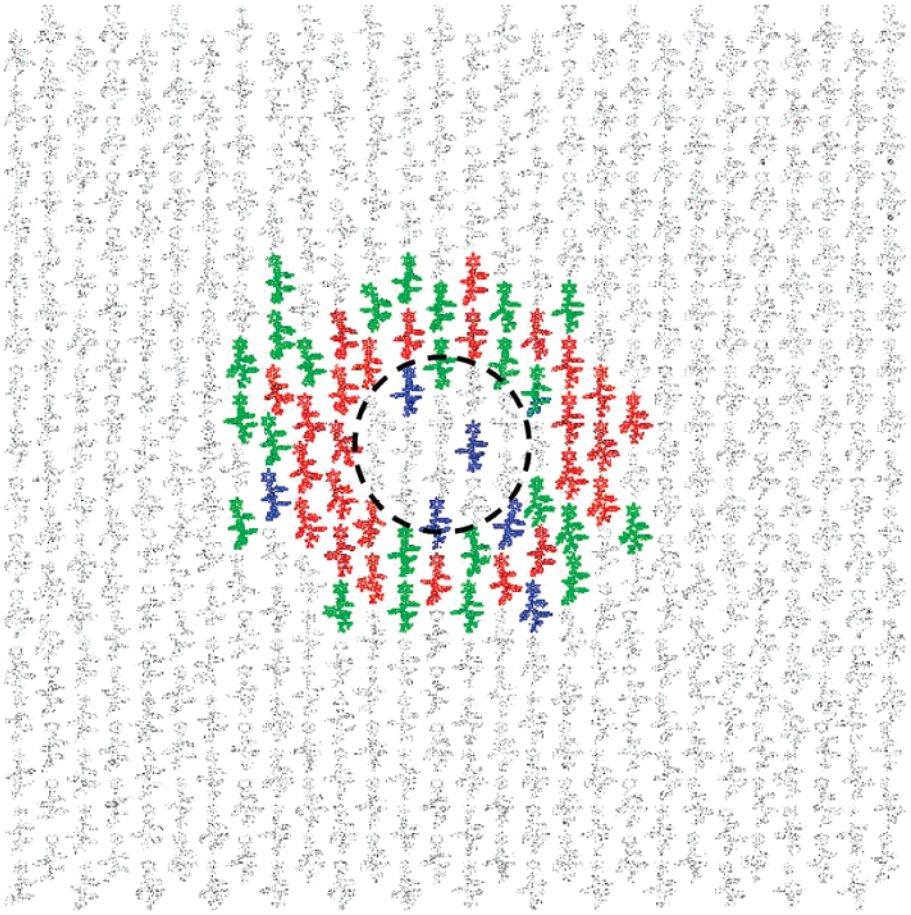

**Figure 8.** Initial locations of PS4 molecules ejected with a kinetic energy higher than 30 eV (red), lower than 30 but greater than 2 eV (green), and less than 2 eV (blue) by 15 keV $Ar_{9000}$ bombardment at normal incidence. Grey spheres depict PS4 molecules that were not sputtered from the surface. The dashed circle represents a vertical projection of the periphery of the $Ar_{9000}$ projectile on the surface.

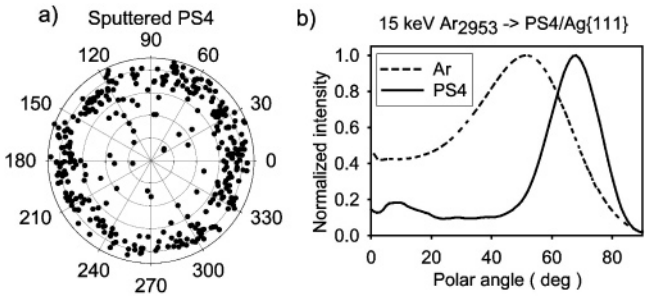


**Figure 9.** Azimuthal (a) and polar angle distributions (b) of intact PS4 molecules (solid line) and Ar atoms (dashed line) ejected by 15 keV $Ar_{2953}$ bombardment of the PS4/Ag{111} system at normal incidence. Points shown on the panel a depict PS4 molecules collected on a flat detector located in front of the sample.

molecules from thin organic overlayers has been also reported for small clusters such as $C_{60}$.[23] The effect was attributed to a catapult-like mechanism of molecular ejection taking place during an opening of a substrate crater.[23] Because the substrate is not altered by 15 keV $Ar_{2953}$, this mechanism is evidently not applicable in the present case. Strong off-normal ejection of PS4 molecules could be attributed to a blocking effect of a dense cloud of incoming Ar atoms.[35,64] Such a cloud would prevent the ejection of particles in directions close to the surface normal. The process is definitely important; however, as it will be shown in the next section, it can only partially account for the observed effect. Strong off-normal ejection of molecular species can generate problems for the detection of neutral molecules as most of the sputtered material will not be recorded with detectors having limited acceptance angles. This problem can be significantly reduced if the sample is bombarded at an off-normal angle and the detector is positioned at a specular azimuthal direction. Strong off-normal ejection will not be as important for the detection of secondary ions, as a strong electric field applied between the sample and the extraction optics will attract all sputtered ions toward the detector.

Finally, it should be pointed out that the polar angle distributions presented in Figure 9 also do not support a concept of molecular entrainment. The angular distribution of PS4 molecules peaks at a much larger angle (around 70°) than the spectrum of Ar atoms. Both these distributions should peak at similar angles, if the entrainment model was to account for molecular ejection.

**Mechanisms.** As was already demonstrated in the previous sections, the physics of molecular ejection by large and slow clusters is distinct from the ejection events stimulated by clusters such as $C_{60}$, $Au_3$, or $SF_5$. The time dependence of the interaction forces between Ar−PS4, Ar−Ag, and PS4−PS4 molecules is calculated to provide additional insight into these processes. The results are presented in Figure 10. The forces are calculated for a selected test molecule being ejected with a high kinetic energy (molecule 1 in Figure 10a). For this molecule, force components along the *x*- and *y*-axis are similar; therefore, only the lateral components along the *x*-axis and the vertical components of forces are shown. From Figure 10b, it is evident that the molecule is accelerated predominantly by interaction with Ar atoms. The acceleration is not caused by separate collisions but is a continuous process stimulated collectively by many Ar

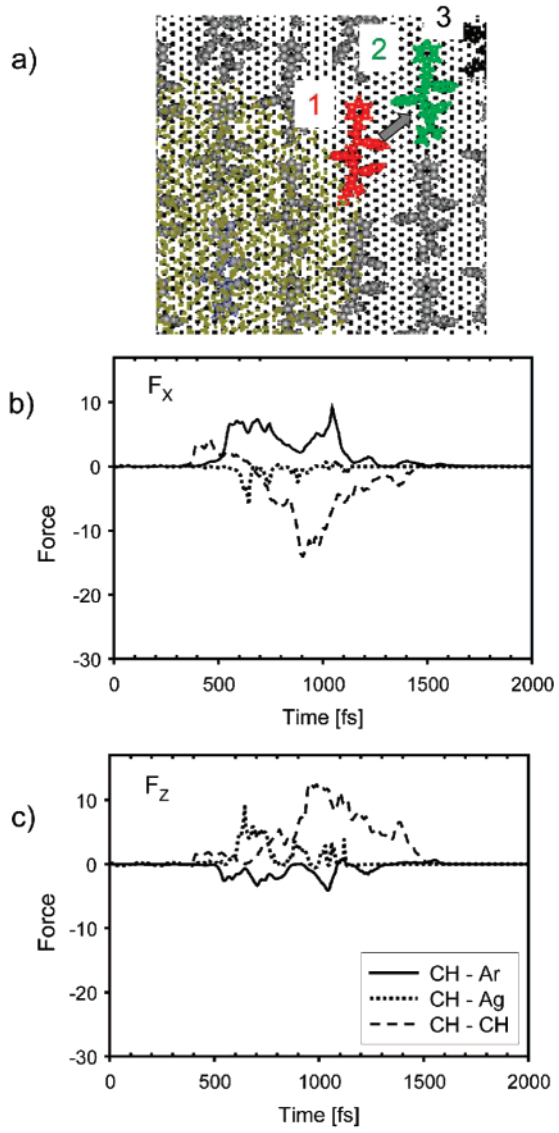


**Figure 10.** Ejection of two PS4 molecules. (a) Top down view of molecules involved in the mechanism. Molecule 1 is red, molecule 2 is green, and molecule 3 (black) is at the upper corner of the figure. (b) Time dependence of the lateral component (*x*-axis) of the force exerted on the test molecule 1 by Ar (solid line), silver atoms (dotted line), and other PS4 molecules (dashed line). (c) Time dependence of the vertical (*z*-axis) component of the force exerted on molecule 1.

atoms passing over a PS4 molecule. It is interesting to note that at no time is the vertical component of the Ar−CH interaction directed toward the vacuum. In other words, back-reflected Ar atoms are not able to uplift the test molecule, but rather, they are pressing it toward the surface, while accelerating it away from the point of impact. After 400 fs beyond the ion impact, the test molecule begins to move along the substrate in the direction shown by an arrow in Figure 10a. At 700 fs, it comes into contact with its nearest neighbor molecule located further away from the point of projectile impact (molecule 2 in Figure 10a). As the molecules begin to interact, a strong vertical component appears in the force, which pushes the test molecule into the vacuum. In other words, the molecule number 2 plays a role of a takeoff board, uplifting its incoming partner as illustrated in Figure 11. There is also an interaction between the test molecule and the substrate, which contributes to the molecular ejection as shown in Figure 10c. However, it is also evident from Figure 10 that the effect of this interaction is much smaller than the effect of the PS4−PS4 force.

A similar process leads to the ejection of a molecule 2. The ejection is predominantly stimulated by interactions with a neighbor molecule located further away from the point of impact (black molecule 3) in a mechanism similar to that noted previously. However, in this case, the ejecting molecule is not accelerated by interaction with projectile atoms but by interactions with molecule 1. Since this molecule has a lower velocity than the Ar atoms, the final energy of ejected molecule 2 is also lower. This chain-like process may continue further. However, because a limited amount of the energy is involved in this process, the sequence of PS4−PS4 collisions is short and involves usually no more than two to three molecules.

The interaction between Ar and PS4 molecules is an initial driving force for molecular ejection as illustrated in Figure 10. However, this interaction must occur at a specific location to lead to the ejection of a molecule. The molecule must reside at the surface at the periphery of the incoming cluster to have a chance for ejection. In this region, backreflected Ar atoms have a strong lateral component of momentum that may accelerate molecules to a high velocity. This process alone is, however, not sufficient, and the interaction with other organic molecules or the deformed substrate is also necessary to eject molecules as shown in Figure 11. Because of intermolecular interactions, the primary energy is distributed to more distant molecules. However, if the molecule is located too far away, the transferred energy is too low, and no ejection occurs. As the amount of available kinetic energy is comparable for all projectiles having the same primary kinetic energy per atom, the length of the chain of intermolecular collisions, and consequently, the thickness of the swept ring-like area, should be more or less similar. Therefore, only the diameter of the altered area should change with the cluster size. This observation explains why there may be a linear dependence between the PS4 sputtering yield and the cluster radius.

As shown in Figure 1, most of the molecules are ejected from a ring-like area starting close to the perimeter of the Ar projectile. Surprisingly, there is almost no ejection from the area located below the projectile. Although the energy delivered to this region is large, the momentum is directed toward the surface. As a result, the molecules are pressed toward the substrate, and no lateral acceleration is present. Even if the molecule obtains a momentum directed toward the vacuum, it cannot penetrate through a dense flux of incoming Ar atoms. The ejection can occur only when the cloud of projectile atoms is sufficiently dispersed to let PS4 molecules pass through. As a result, the ejection by this channel can occur very late in the trajectory. Our calculations indicate that some of the molecules are ejected from the area below the impinging cluster. However, as shown in Figure 12, Ar−PS4 interactions are not a driving force for molecular emission in this case. Organic molecules originally located below the cluster are ejected by collective interaction with the recovering substrate, which acts as a trampoline hurling the molecule into the vacuum. Since this process has a low rate, the molecules are ejected with a very low kinetic energy. A similar mechanism has been proposed to explain the ejection of benzene molecules deposited on a graphite surface stimulated by an impact of low-energy $C_{60}$ projectiles.[19] Our calculations are performed with the assumption that all particles have zero velocities at time $t = 0$ fs. The effect of finite temperature is coupled with the adhesion energy of the molecules to the surface, which in these simulations is relatively large. As a result, the thermal movements should have only a minor effect on the ejection of high-energy PS4 molecules, which compose a majority of ejected flux. These

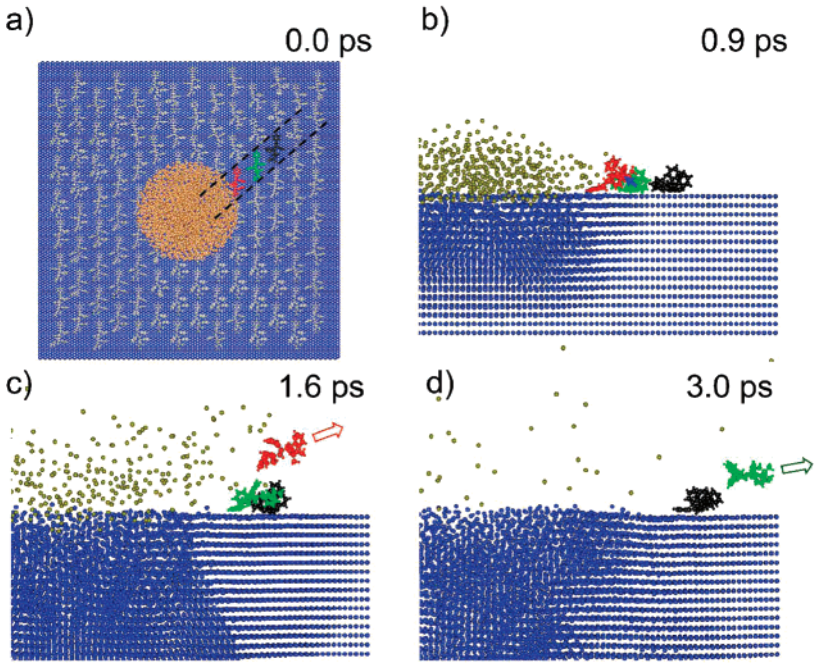


**Figure 11.** Time evolution of the ejection of high- and medium-energy PS4 molecules induced by 15 keV $Ar_{2953}$ cluster impact at normal incidence. Panel a represents a top view of the system before cluster impact. Panels b−d display particles located within a slice 1.5 nm wide centered at the point of impact. The orientation of the slice is schematically marked by dashed lines in panel a. Only colored molecules from panel a are shown. The arrows indicate a final direction of a momentum of ejected PS4 molecules.

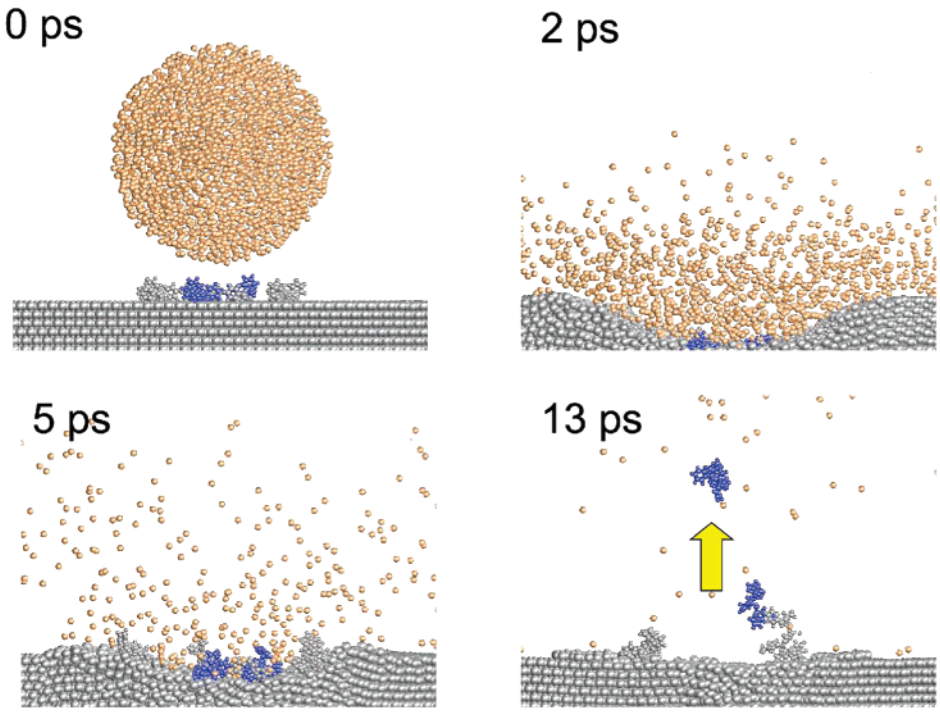


**Figure 12.** Time evolution of the ejection of low-energy PS4 molecules induced by 15 keV $A_{2953}$ cluster impact at normal incidence. Only ejected molecules together with their nearest neighbor molecules located within a slice 1.5 nm wide centered at the point of impact are shown.

molecules are initially strongly bound to the surface, and the kinetic energy transferred in collisions significantly exceeds the energy deposited in thermal vibrations. However, thermal vibrations may have some influence on the ejection of low-energy molecules. This interesting effect will be investigated in the future.

The final issue that should also be addressed is the universality of the presented mechanism. The model is proposed to explain results of sputtering of a molecular monolayer composed of relatively flat molecules that are strongly bound to the surface. As the molecules become more protruding or the bombarded layer becomes thicker, the direct side interactions between the expanding Ar cluster and the organic material should have a vertical component of the force directed away from the surface. As a result, interactions between Ar atoms and organic molecules should directly lead to the ejection of organic molecules. In this case, one should expect that the sputtering yield should continue to rise up to a larger kinetic energy per atom because more material can be removed if more energy will be delivered to the system. The ejection of molecules will

be also enhanced if the binding between the molecule and the surface weakens. In this case, one can expect that, in particular, more low-energy molecules will be emitted from the area located below the cluster. As a result, the ejection area should transform from a ring-like shape into a circle. A natural consequence of such a change should be a deviation from a linear dependence between the molecular sputtering yield and the radius of the bombarding cluster. Finally, the proposed model can be applied to noble-gas or other weakly bound clusters only. If the atoms in the cluster are more strongly bound, they would require a larger kinetic energy per atom to become side-jetted. A larger kinetic energy will, in turn, lead to the ejection of substrate atoms and, consequently, to a larger contribution of processes already known from the desorption of organic films stimulated by a small, energetic cluster bombardment.

## 4. Conclusion

The processes of molecular ejection from thin organic overlayers adsorbed on a metal substrate stimulated by slow, large noble-gas cluster projectiles were investigated. It was found that below a critical primary kinetic energy, the emission characteristics are distinctly different from those stimulated by atomic and small cluster impacts. The emission of intact organic molecules is very efficient even if no substrate atoms are ejected. A significant number of molecules was ejected with an unexpectedly high kinetic energy at almost oblique polar angles. The yield increases strongly with the primary kinetic energy above a certain threshold energy and then saturates. The yield also increases with the size of the cluster projectile having the same kinetic energy per atom. However, if the total primary kinetic energy is constant, the molecular sputtering yield has a maximum at a specific cluster size. The position of this maximum depends on the primary kinetic energy. Finally, the total yield of organic molecules depends weakly on the angle of incidence.

A novel desorption mechanism was proposed to explain the observed phenomena. In this model, the ejection of intact molecules is initiated by direct interactions between organic molecules and backreflected projectile atoms, provided that these atoms have a sufficient lateral component of momentum. Such interactions occur also during atomic or small cluster bombardment. In these cases, however, the sputtering yield generated by direct collisions is small because the lateral component of momentum is missing. Furthermore, these collisions are quite energetic, and the process leads almost entirely to the ejection of molecular fragments. The energy transferred from Ar atoms to the molecular overlayer is further dispersed by intermolecular collisions. The collision sequence is short. As a result, the molecules are ejected from a ring-like area. The size of this area is directly related to the size of the projectile. Contrary to the desorption scenarios proposed to describe the erosion of thin organic overlayers by atomic or small cluster projectiles, during slow and large noble-gas cluster bombardment, the energized substrate plays only a minor role in the ejection of intact organic species. If the kinetic energy of the projectile is not sufficient to form a crater in the substrate, only a few molecules are ejected by a direct substrate−PS4 interaction. These molecules are ejected not by interaction with individual substrate atoms as takes place during atomic or small cluster bombardment but by a collective action from the recovering substrate. This process leads to the ejection of organic molecules with a very low translational kinetic energy.

The observations presented in this paper provide insight into the efficacy of slow, large noble-gas cluster beams for molecular desorption in TOF−SIMS experiments. There are several features that indicate that the application of such projectiles could be potentially useful for SIMS/SNMS analysis of thin organic overlayers deposited on an inorganic substrate. First, a large molecular signal is generated by the impact of a single projectile. This observation differs from measurements performed with small cluster projectiles, where the signal is usually low and no significant yield enhancement is reported when the atomic projectile is replaced by a small cluster ion.[2,6,65] The efficiency of molecular ejection increases with the size of the cluster, provided that a constant energy per atom can be secured. At the same time, the onset for molecular desorption is shifted toward a lower kinetic energy per atom. Lowering of the desorption threshold results in the ejection of less internally excited molecules and, consequently, to a lower fragmentation of molecules on their way to the detector. All these observations indicate that a primary beam composed of the largest available clusters should be used to probe organic overlayers. Bombardment by a larger cluster results also in a larger number of Ar atoms having a chance to collectively interact with the organic molecule. A cumulative action of a larger number of projectile atoms should, in turn, allow uplifting larger molecules. As a result, the application of such projectiles could potentially allow the detection of higher molecular weight molecules.[31] Another potentially positive feature of large cluster ion beams is the ability to collect spectra without fragments. This ability could, in some cases, simplify the procedure of chemical identification of analyzed material. However, if the presence of specific fragments is necessary to accomplish more elaborate chemical identification, it can be achieved by a simple increase of the kinetic energy of the primary beam.

**Acknowledgment.** Financial support from the Polish Ministry of Science and Higher Education (Programs PB4097/H03/2007/33 and PB2030/H03/2006/31) and the National Science Foundation (Grants CHE-045614 and CHE-555314) are gratefully acknowledged. The Academic Services and Emerging Technologies group at Penn State provided us early access to the lion-xo PC cluster.

## References and Notes

(1) Castner, D. G. *Nature (London, U.K.)* **2003**, *422*, 129.
(2) Winograd, N. *Anal. Chem.* **2005**, *77*, 142 and references therein.
(3) Kotter, F.; Benninghoven, A. *Appl. Surf. Sci.* **1998**, *133*, 47.
(4) Sun, S.; Szakal, C.; Roll, T.; Mazarov, P.; Wucher, A.; Winograd, N. *Surf. Interface Anal.* **2004**, *36*, 1367.
(5) Szakal, C.; Sun, S.; Wucher, A.; Winograd, N. *Appl. Surf. Sci.* **2004**, *231−232*, 183.
(6) Sostarecz, A. G.; Sun, S.; Szakal, C.; Wucher, A.; Winograd, N. *Appl. Surf. Sci.* **2004**, *231−232*, 179.
(7) Sun, S.; Wucher, A.; Szakal, C.; Winograd, N. *Appl. Phys. Lett.* **2004**, *84*, 5177.
(8) Wucher, A.; Sun, S.; Szakal, C.; Winograd, N. *Appl. Surf. Sci.* **2004**, *231−232*, 68.
(9) Wucher, A.; Sun, S. X.; Szakal, C.; Winograd, N. *Anal. Chem.* **2004**, *76*, 7234.
(10) Haberland, H.; Insepov, Z.; Moseler, M. *Phys. Rev. B: Condens. Matter Mater. Phys.* **1995**, *51*, 11061.
(11) Aoki, T.; Seki, T.; Matsuo, J.; Insepov, Z.; Yamada, I. *Mater. Chem. Phys.* **1998**, *54*, 139.
(12) Seki, T.; Aoki, T.; Tanomura, M.; Matsuo, J.; Yamada, I. *Mater. Chem. Phys.* **1998**, *54*, 143.
(13) Webb, R.; Kerford, M.; Way, A.; Wilson, I. *Nucl. Instrum. Methods Phys. Res., Sect. B* **1999**, *153*, 284.
(14) Garrison, B. J.; Delcorte, A.; Krantzman, K. D. *Acc. Chem. Res.* **2000**, *33*, 69.
(15) Delcorte, A.; Vanden Eynde, X.; Bertrand, P.; Vickerman, J. C.; Garrison, B. J. *J. Phys. Chem. B* **2000**, *104*, 2673.
(16) Colla, T. J.; Aderjan, R.; Kissel, R.; Urbassek, H. M. *Phys. Rev. B: Condens. Matter Mater. Phys.* **2000**, *62*, 8487.

(17) Aderjan, R.; Urbassek, H. M. *Nucl. Instrum. Methods Phys. Res., Sect. B* **2000**, *164*, 697.
(18) Nguyen, T. C.; Ward, D. W.; Townes, J. A.; White, A. K.; Krantzman, K. D.; Garrison, B. J. *J. Phys. Chem. B* **2000**, *104*, 8221.
(19) Webb, R.; Kerford, M.; Ali, E.; Dunn, M.; Knowles, L.; Lee, K.; Mistry, J.; Whitefoot, F. *Surf. Interface Anal.* **2001**, *31*, 297.
(20) Postawa, Z.; Czerwinski, B.; Szewczyk, M.; Smiley, E. J.; Winograd, N.; Garrison, B. J. *Anal. Chem.* **2003**, *75*, 4402.
(21) Postawa, Z.; Czerwinski, B.; Szewczyk, M.; Smiley, E. J.; Winograd, N.; Garrison, B. J. *J. Phys. Chem. B* **2004**, *108*, 7831.
(22) Anders, C.; Urbassek, H. M.; Johnson, R. E. *Phys. Rev. B: Condens. Matter Mater. Phys.* **2004**, *70*.
(23) Postawa, Z.; Czerwinski, B.; Winograd, N.; Garrison, B. J. *J. Phys. Chem.* **2005**, *109*, 11973.
(24) Anders, C.; Urbassek, H. M. *Nucl. Instrum. Methods Phys. Res., Sect. B* **2005**, *228*, 84.
(25) Krantzman, K. D.; Kingsbury, D. B.; Garrison, B. J. *Nucl. Instrum. Methods Phys. Res., Sect. B* **2007**, *255*, 238.
(26) Kerford, M.; Webb, R. P. *Nucl. Instrum. Methods Phys. Res., Sect. B* **1999**, *153*, 270.
(27) Colla, T. J.; Urbassek, H. M. *Nucl. Instrum. Methods Phys. Res., Sect. B* **2000**, *164*, 687.
(28) Czerwinski, B.; Delcorte, A.; Garrison, B. J.; Samson, R.; Winograd, N.; Postawa, Z. *Appl. Surf. Sci.* **2006**, *252*, 6419.
(29) Anders, C.; Sebastian, M.; Urbassek, H. M. *Surf. Sci.* **2006**, *600*, 2587.
(30) Mahoney, J. F.; Perel, J.; Lee, T. D.; Martino, P. A.; Williams, P. *J. Am. Soc. Mass Spectrom.* **1992**, *3*, 311.
(31) Cornett, D. S.; Lee, T. D.; Mahoney, J. F. *Rapid Commun. Mass Spectrom.* **1994**, *8*, 996.
(32) Beuhler, R. J.; Friedman, L. *Int. J. Mass Spectrom. Ion Processes* **1989**, *94*, 25.
(33) Novikov, A.; Caroff, M.; Della-Negra, S.; Depauw, J.; Fallavier, M.; Le Beyec, Y.; Pautrat, M.; Schultz, J. A.; Tempez, A.; Woods, A. S. *Rapid Commun. Mass Spectrom.* **2005**, *19*, 1851.
(34) Guillermier, C.; Della Negra, S.; Rickman, R. D.; Pinnick, V.; Schweikert, E. A. *Appl. Surf. Sci.* **2006**, *252*, 6529.
(35) Yamada, I.; Matsuo, J.; Insepov, Z.; Aoki, T.; Seki, T.; Toyoda, N. *Nucl. Instrum. Methods Phys. Res., Sect. B* **2000**, *164*, 944.
(36) Yamada, I.; Matsuo, J.; Toyoda, N.; Ion, C. R. C. C. *Nucl. Instrum. Methods Phys. Res., Sect. B* **2003**, *206*, 820 and references therein.
(37) Matsuo, J.; Okubo, C.; Seki, T.; Aoki, T.; Toyoda, N.; Yamada, I. *Nucl. Instrum. Methods Phys. Res., Sect. B* **2004**, *219*−*220*, 463.
(38) Ninomiya, S.; Nakata, Y.; Ichiki, K.; Seki, T.; Aoki, T.; Matsuo, J. *Nucl. Instrum. Methods Phys. Res., Sect. B* **2007**, *256*, 493.
(39) Hiraoka, K.; Asakawa, D.; Fujimaki, S.; Takamizawa, A.; Mori, K. *Eur. Phys. J. D* **2006**, *38*, 225.
(40) Takats, Z.; Wiseman, J. M.; Gologan, B.; Cooks, R. G. *Science (Washington, DC, U.S.)* **2004**, *306*, 471.
(41) Takats, Z.; Wiseman, J. M.; Cooks, R. G. *J. Mass Spectrom.* **2005**, *40*, 1261.
(42) Haller, K. K.; Ventikos, Y.; Poulikakos, D.; Monkewitz, P. *J. Appl. Phys.* **2002**, *92*, 2821.
(43) Cleveland, C. L.; Landman, U. *Science (Washington, DC, U.S.)* **1992**, *257*, 355.
(44) Aoki, T.; Matsuo, J.; Insepov, Z.; Yamada, I. *Nucl. Instrum. Methods Phys. Res., Sect. B* **1997**, *121*, 49.
(45) Zimmermann, S.; Urbassek, H. M. *Phys. Rev. A: At., Mol., Opt. Phys.* **2006**, *74*, 63203.
(46) Aoki, T.; Matsuo, J. *Nucl. Instrum. Methods Phys. Res., Sect. B* **2007**, *257*, 645.
(47) Garrison, B. J. Molecular dynamics simulations, the theoretical partner to static SIMS experiments. In *TOF-SIMS: Surface Analysis by Mass Spectrometry*; Vickerman, J. C., Briggs, D., Eds.; Surface Spectra: Manchester, U.K., 2001; p 223.
(48) Kelchner, C. L.; Halstead, D. M.; Perkins, L. S.; Wallace, N. M.; Depristo, A. E. *Surf. Sci.* **1994**, *310*, 425.
(49) Wilson, W. D.; Haggmark, L. G. *Phys. Rev. B: Condens. Matter Mater. Phys.* **1977**, *15*, 2458.
(50) Aziz, R. A.; Slaman, M. J. *Mol. Phys.* **1986**, *58*, 679.
(51) Stuart, S. J.; Tutein, A. B.; Harrison, J. A. *J. Chem. Phys.* **2000**, *112*, 6472.
(52) Brenner, D. W.; Shenderova, O. A.; Harrison, J. A.; Stuart, S. J.; Ni, B.; Sinnott, S. B. *J. Phys.: Condens. Matter* **2002**, *14*, 783.
(53) Postawa, Z.; Ludwig, K.; Piaskowy, J.; Krantzman, K.; Winograd, N.; Garrison, B. J. *Nucl. Instrum. Methods Phys. Res., Sect. B* **2003**, *202*, 168.
(54) Adelman, S. A.; Doll, J. D. *J. Chem. Phys.* **1974**, *61*, 4242.
(55) Beeler, J. R. *Radiation Effects Computer Experiments*; 1983.
(56) Garrison, B. J.; Kodali, P. B. S.; Srivastava, D. *Chem. Rev.* **1996**, *96*, 1327.
(57) Moseler, M.; Nordiek, J.; Haberland, H. *Phys. Rev. B: Condens. Matter Mater. Phys.* **1997**, *56*, 15439.
(58) Wucher, A.; Garrison, B. J. *Phys. Rev. B: Condens. Matter Mater. Phys.* **1992**, *46*, 4855.
(59) Wucher, A.; Garrison, B. J. *J. Chem. Phys.* **1996**, *105*, 5999.
(60) Chatterjee, R.; Postawa, Z.; Winograd, N.; Garrison, B. J. *J. Phys. Chem. B* **1999**, *103*, 151.
(61) Russo, M. F., Jr.; Szakal, C.; Kozole, J.; Winograd, N.; Garrison, B. J. *Anal. Chem.* **2007**, *79*, 4493.
(62) Russo, M. F., Jr.; Garrison, B. J. *Anal. Chem.* **2006**, *78*, 7206.
(63) Zhigilei, L. V.; Garrison, B. J. *Rapid Commun. Mass Spectrom.* **1998**, *12*, 1273.
(64) Toyoda, N.; Kitani, H.; Hagiwara, N.; Aoki, T.; Matsuo, J.; Yamada, I. *Mater. Chem. Phys.* **1998**, *54*, 262.
(65) Weibel, D.; Wong, S.; Lockyer, N.; Blenkinsopp, P.; Hill, R.; Vickerman, J. C. *Anal. Chem.* **2003**, *75*, 1754.